

# Selectivity in the Polymerization of Olefins with Cyclopentadienyl Chromium Catalysts: A Density Functional Study

Curtis W. Hoganson,<sup>†</sup> Douglas J. Doren,\* and Klaus H. Theopold

Department of Chemistry and Biochemistry and Center for Catalytic Science and Technology, University of Delaware, Newark, Delaware 19716

Received July 25, 2003; Revised Manuscript Received October 19, 2003

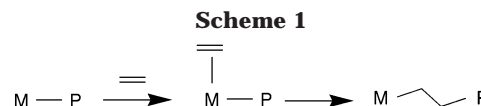
**ABSTRACT:** The chromium-based Union Carbide catalyst exhibits high activity for the homopolymerization of ethylene. However, it fails to catalyze the homopolymerization of  $\alpha$ -olefins or even the copolymerization of the latter with ethylene. To understand the origins of this selectivity, density functional theory calculations are used to model the olefin polymerization reactions of a cyclopentadienylchromium-(III) complex whose properties recommend it as a structural and functional model for the Union Carbide catalyst. We find that this chromium alkyl binds both ethylene and propene weakly and therefore reversibly, and that the barrier for insertion of propene is significantly higher than that for inserting ethylene. Because olefin binding is reversible, the insertion step discriminates against the incorporation of  $\alpha$ -olefin into the polymer chain.

## Introduction

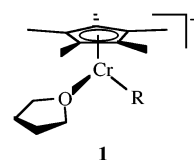
Polyolefins, including polyethylene, have become ubiquitous materials, whose microstructure and attendant properties depend greatly on the polymerization catalyst used for their production. The promise of improved control of polymer properties has led to intense research efforts in industry and academia devoted to the discovery of novel catalysts and to the elucidation of the reaction mechanisms. Among the commercially used heterogeneous catalysts containing chromium, two types are especially notable. These are the Phillips catalyst,<sup>1</sup> consisting of inorganic chromium on a silica support, and the Union Carbide catalyst,<sup>2</sup> prepared by depositing chromocene (i.e.  $(\eta^5\text{-C}_5\text{H}_5)_2\text{Cr}$ ) on silica. An important distinction is that the Union Carbide catalyst does not homopolymerize  $\alpha$ -olefins and effects very little incorporation of  $\alpha$ -olefin in copolymerizations with ethylene. The Phillips catalyst does not share this limitation. The present theoretical study concerns a homogeneous model system for the Union Carbide catalyst that faithfully reproduces this discrimination between ethylene and higher olefins.<sup>3,4</sup> The aim is to identify the origins of the high ethylene/propene selectivity ratio of cyclopentadienylchromium catalysts.

The mechanism by which transition metal complexes catalyze olefin polymerization has been studied extensively by theoretical means,<sup>5,6</sup> and these studies provide unambiguous support for the previously formulated Cossee mechanism (Scheme 1).<sup>7</sup> Agostic interactions between the metal atom and the C–H bonds of the alkyl group (or polymer chain) often play an important role by stabilizing ground and/or transition states along the reaction pathway.<sup>8</sup>

While ethylene polymerization has been the subject of many computational studies, including some recent papers dealing explicitly with chromium-containing catalysts,<sup>9,10,11</sup> propene polymerization has been less frequently studied by computational means,<sup>6,12,13</sup> and the concern is usually to understand the stereochemis-



try of the resulting polymer. The goal of this work is to suggest an explanation for the high ethylene/propene reactivity ratio ( $r_1$ ) of cyclopentadienylchromium catalysts like the Union Carbide catalysts ( $r_1 = 72$  at 90 °C).<sup>2</sup> The calculations exploit the availability of an experimentally well-characterized homogeneous model system, the organometallic compound  $[\text{Cp}^*\text{Cr}(\text{THF})_2\text{CH}_3]\text{BPh}_4$  (**1**,  $\text{Cp}^* = \eta^5\text{-C}_5\text{Me}_5$ , THF = tetrahydrofuran).<sup>14</sup>



In  $\text{CH}_2\text{Cl}_2$  solution, this chromium(III) alkyl catalyzes the polymerization of ethylene at ambient temperature and pressure. Inhibition of the polymerization by THF indicates that dissociation of one of the THF ligands of **1** generates the actual polymerization catalyst, namely the coordinatively unsaturated 13-electron cation  $[\text{Cp}^*\text{Cr}(\text{THF})\text{CH}_3]^+$ . **1** does not catalyze the polymerization of propene and in attempted ethylene/propene copolymerizations it produces regular polyethylene without detectable methyl branching. If anything, the selectivity ratio of the model compound is thus even higher than that of the heterogeneous catalyst; the larger and more electron-donating  $\text{Cp}^*$ -ligand may be the source of this difference.

The ethylene/propene discrimination might originate in either the olefin binding step or in the transition state for its insertion. In either case the discrimination may be steric or electronic in origin. To address these questions we have performed hybrid density functional theory (DFT) calculations to model the structures and to estimate the energies of the intermediates and transition states of the reactions with both ethylene and propene. We have also varied the length of the alkyl

\* Corresponding author. E-mail: doren@udel.edu.

<sup>†</sup> Present address: Department of Chemistry, Ursinus College, P.O. Box 1000, Collegeville, PA 19426.

chain bound to the chromium, replacing the methyl with a propyl group, to better approximate a growing polymer chain and to examine the effect on the reaction energetics.

## Models and Methods

The calculations reported here use simplified versions of the homogeneous model catalyst **1**, such as  $[\text{CpCr}(\text{THF})_2\text{CH}_3]^+$  (in the following the invariant  $\text{CpCr}(\text{THF})$  moiety will be denoted by **Cr**; thus, the computational model for **1** becomes  $[\text{Cr}(\text{THF})\text{Me}]^+$ ). Here, the  $\text{Cp}^*$  ring of **1** has been replaced by a cyclopentadienyl ( $\text{Cp} = \eta^5\text{-C}_5\text{H}_5$ ) ring, and the tetraphenylborate counterion has been omitted. Although these changes are likely to have some effect on geometric parameters and energies, the simplifications are reasonable for our initial investigations of this system. In particular, the counteranion is noncoordinating and will only exhibit weak interactions with the catalyst. Moreover, as far as the cyclopentadienyl ring is concerned, these calculations may be more relevant to the heterogeneous Union Carbide catalyst, which features a Cp ligand. In addition to  $[\text{Cr}(\text{THF})\text{Me}]^+$ , we have also considered  $[\text{Cr}(\text{THF})\text{Pr}]^+$ , an analogue with the methyl ligand (Me) replaced by a propyl group (Pr), to more realistically model the growing polymer chain.

The DFT calculations were carried out with Gaussian98,<sup>15</sup> using the hybrid B3LYP functional.<sup>16,17</sup> Compact effective core potential basis sets were used for all non-hydrogen atoms.<sup>18,19</sup> The double- $\zeta$  cep-31 g basis set was used for geometry optimizations, frequency calculations and estimates of solvation energy. Energies at the optimized geometries were determined with the larger triple- $\zeta$  cep-121 g\*\* basis set, including polarization functions on all atoms except chromium. In general, the relative energies obtained using the smaller basis set corresponded very well to those obtained with the larger. Three representative structures, two minima and one transition state, were reoptimized using the larger basis set, and only small changes in the structures and energies were found.

Normal-mode analyses were used to confirm that each of the transition states had a single unstable mode, and to provide estimates of the vibrational energies and entropies of all the complexes. All low frequency modes were treated as harmonic vibrations in calculating zero-point energies and thermodynamic quantities. Inclusion of vibrational energies (zero point plus thermal energy) makes only a small contribution to the reaction energies reported below, and is most important for the olefin-binding step. Solvation effects on free energies were estimated by using a self-consistent reaction field method, the conductor-like screening model.<sup>20</sup> These are also most important for the olefin-binding step. Reaction paths were followed by minimization from the transition state to verify that the path connected the assumed reactants and products.

## Results and Discussion

The calculations reported below are all for the quartet spin state. This is the ground state for all of the Cr(III) complexes discussed here, as it is for other quite similar complexes.<sup>21,22</sup> For the  $\pi$ -complex of ethylene, i.e.,  $[\text{Cr}(\text{C}_2\text{H}_4)\text{Me}]^+$ , we have evaluated the energy of the doublet state at the geometry optimized for the quartet. This was found to be 94 kcal/mol above the quartet, respectively. We have optimized the doublet state geometry of the ethylene  $\pi$ -complex  $[\text{Cr}(\text{C}_2\text{H}_4)\text{Pr}]^+$ , and found it to be 22 kcal/mol above the optimal ground state quartet. Both doublets exhibit spin-contamination, whereas all the quartet states in this study are essentially free from spin contamination. Mulliken population analyses of the quartet states show that the three unpaired electrons are localized on the chromium atom in all of the structures discussed here.

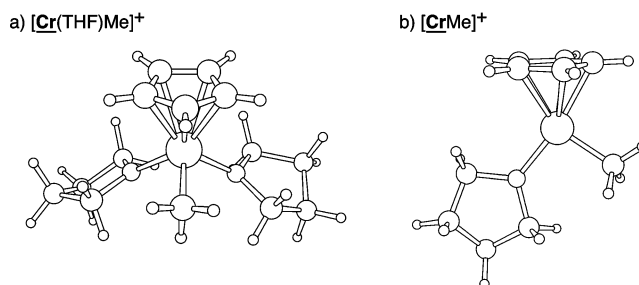
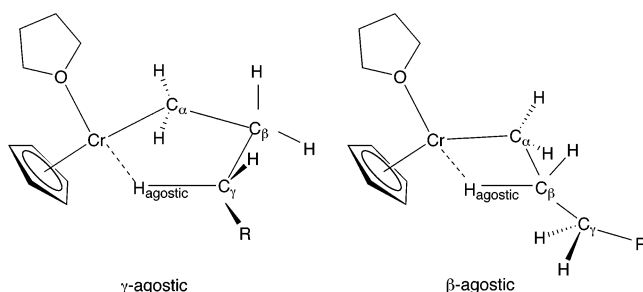


**Figure 1.** Optimized structures of (a)  $[\text{CpCr}(\text{THF})_2\text{CH}_3]^+$  and (b)  $[\text{CpCr}(\text{THF})\text{CH}_3]^+$ .

To compare the reactions of  $[\text{Cr}(\text{THF})\text{Me}]^+$  and  $[\text{Cr}(\text{THF})\text{Pr}]^+$  with either ethylene or propene, we have optimized structures relevant to all four of these reactions. Most of these complexes may adopt a large number of conformations (e.g., we count 216 for the propene complex  $[\text{Cr}(\text{C}_3\text{H}_6)\text{Pr}]^+$ ), many of which are expected to have similar energies. Rather than attempting to optimize all of these conformations, we have examined a small subset. For example, the puckered THF ring can adopt two conformations, but in the reported structures, the out-of-plane twist of this ring always has the same sense. Similarly, all propyl groups have *anti* conformations in the reported structures. The insertion transition states have been explored in some detail, as have the ethylene  $\pi$ -complexes. The structures of the propene  $\pi$ -complexes and of the products of insertion, however, are of greatest interest when they derive from the most relevant insertion transition structures, that is, when they can be reached directly by descending along the energy gradient from the transition structure of lowest energy. The structural and energetic data presented below are for these structures only. In the following subsections, we first describe the structures involved and then the energetics of the reaction sequences.

**Chromium Alkyls: Precursor and Active Catalyst.** The optimized structure of the precursor complex  $[\text{Cr}(\text{THF})\text{Me}]^+$ , shows a “three-legged piano stool” geometry (Figure 1a). Selected bond lengths and angles of this precursor complex are given in the Supporting Information, along with analogous data for **1**,  $[\text{Cp}^*\text{Cr}(\text{THF})_2\text{CH}_3]\text{BPh}_4$ , obtained by X-ray crystallography.<sup>14</sup> The calculated Cr–O and Cr–C<sub>Me</sub> bond lengths are in good agreement with the experimentally determined numbers. The calculated Cr–C<sub>Cp</sub> bond lengths are slightly longer than the measured Cr–C<sub>Cp</sub> values and exceed the average Cr–C<sub>Cp</sub> distance (2.225 Å) by a significant margin. This may reflect the difference between the crystal (for the experiment) and gas phase (for the calculation) environments. The calculated bond lengths within the THF ligands are also longer than observed in **1**, though this may be due to the nature of the measurement, rather than an error in the calculation. The calculated bond lengths are close to the values in free THF. Indeed, it has previously been noted that the C–C bond distances in the THF ring as determined in the X-ray structure of **1** are unusually short, and that this may be an artifact of dynamic disorder.<sup>14</sup> The THF ligands are puckered, with C–C–C–C dihedral angles of about 39°. Normal-mode analysis shows that inversion of the THF ring has a low frequency, 240 cm<sup>−1</sup>. The X-ray structure shows large thermal ellipsoids for the THF carbons, consistent with either dynamic or static conformational heterogeneity in the crystal. Neither THF nor Cp are directly involved in the reaction, so we

Chart 1



do not expect these small discrepancies in structure to impact directly on the relative reactivity of different olefins. The angles between the three monodentate ligands are around  $94^\circ$ , consistent with a pseudooctahedral structure for the  $d^3$  ion.

Loss of one THF from the catalyst precursor  $[\text{Cr}(\text{THF})\text{Me}]^+$  yields the model of the presumed active catalyst  $[\text{CrMe}]^+$  (Figure 1b). The calculated geometry (reported in the Supporting Information) is essentially the same as previously reported in ref 10. This coordinatively unsaturated complex adopts a trigonal geometry, although the angle between the methyl and THF ligands remains at about  $95^\circ$ . The removal of a ligand results in the expected contraction of all the bonds to chromium. Formation of  $[\text{CrMe}]^+$  from  $[\text{Cr}(\text{THF})\text{Me}]^+$  is associated with an estimated  $\Delta E_{298}$  of about +23 kcal/mol (a normal mode calculation on the bis-THF complex was not performed). Ligand dissociation occasions an increase of entropy that would put  $\Delta G_{298}$  at approximately +10–12 kcal/mol. We calculate that solvation in  $\text{CH}_2\text{Cl}_2$  lowers the free energy change for dissociation by an additional 10 kcal/mol. Thus, the dissociation of one THF from the bis-THF complex in solution is expected to be approximately thermoneutral. This result implies that there should be a significant population of the coordinatively unsaturated mono-THF complex, and is consistent with experimental observations of free THF in solution.<sup>14</sup>

Incorporation of the first monomer of ethylene into the “polymer” chain of  $[\text{CrMe}]^+$  gives  $[\text{CrPr}]^+$ , which may adopt conformations containing either a  $\beta$ - or  $\gamma$ -agostic interaction (Chart 1; geometric parameters in Supporting Information).

The  $\gamma$ -agostic complex forms, in effect, a five-membered ring in which adjacent carbon atoms adopt staggered conformations. By contrast, the  $\beta$ -agostic complex forms a four-membered ring with the  $\alpha$  and  $\beta$  carbons eclipsed. The  $\beta$ -agostic complex has a significantly shorter Cr–H distance (1.95 vs 2.21 Å) and is about 4 kcal/mol lower in energy than the  $\gamma$ -agostic complex. We were unable to locate a minimum energy structure containing no agostic interaction, but from the energy of nonoptimized structures, the  $\gamma$ - and  $\beta$ -agostic interactions appear to be worth about 3 and 7 kcal/mol, respectively.

**Olefin Complexes.** The coordinatively unsaturated catalysts  $[\text{CrMe}]^+$  and  $[\text{CrPr}]^+$  can bind a molecule of olefin in a  $\pi$ -complex and thus revert to the pseudooctahedral geometry. The  $\pi$ -complexes of  $[\text{CrPr}]^+$  are geometrically similar to those of  $[\text{CrMe}]^+$  (Table 1), so the discussion will focus on the latter for simplicity. Two positions of the C=C bond of ethylene afford minima of almost equal energy (Figure 2); the olefinic carbon atoms lie nearly in plane with either the Cr–O (A) or the Cr–C<sub>Me</sub> bond (B, Table 3). The subsequent insertion

Table 1. Calculated Bond Lengths (Å) and Angles (deg) of the  $\pi$ -Complexes (Rotamers B)

	[CrMe] <sup>+</sup>		[CrPr] <sup>+</sup>	
	+ethylene	+propene	+ethylene	+propene
Cr–C1	2.577	2.436	2.527	2.468
Cr–C2	2.542	2.808	2.582	2.825
C2–C1	1.377	1.381	1.376	1.380
Cr–C(alkyl)	2.066	2.061	2.076	2.074
C(alkyl)–C2	2.999	3.239	3.163	3.34
Cr–O	2.043	2.051	2.056	2.055
Cr–C1–C2	73.0	90.4	76.6	89.9

reaction follows from conformation B, which has a calculated energy 0.3 kcal/mol higher than that of conformation A. A scan of nonoptimized intermediate structures indicates that the barrier for internal rotation between A and B is less than 3 kcal/mol.

Focusing on the reactive rotamer B, the coordination of ethylene is nearly symmetric, with the Cr–C bond distances differing by less than 0.06 Å. The very slight lengthening of the C=C bond (1.38 vs 1.34 Å in free ethylene) and the essential planarity of the molecule (sum of three adjacent angles in each CCH<sub>2</sub> moiety:  $359.6^\circ$  and  $359.3^\circ$ ) provide no evidence of significant  $\pi$ -back-bonding from the  $d^3$  ion. Average values of these parameters for several conformations are similar (Figure 3a).

The propene  $\pi$ -complexes have more conformational variety. Incorporation of the prochiral  $\alpha$ -olefin into the chiral chromium complex gives rise to two diastereomers, and the presence of the methyl group of propene is expected to confer a stronger steric bias upon the energies of different rotamers (about the Cr–olefin bond). We have not examined the full potential energy surface of these complexes, but it appears that there should be three structures that are local energy minima, largely because they minimize steric interactions between the methyl group of propene and the three other ligands on chromium. Again, only the conformations reached by minimization from the lowest energy transition state for insertion have been considered in detail (Table 1). In contrast to the ethylene  $\pi$ -complexes, the

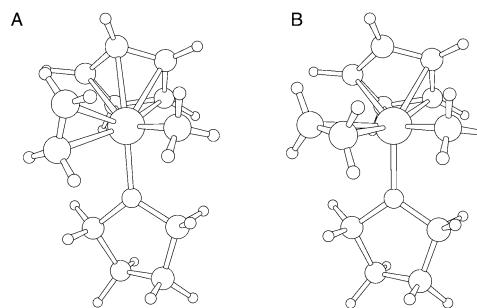


**Figure 2.** Low energy rotamers of the ethylene complex  $[\text{CpCr}(\text{THF})(\text{C}_2\text{H}_4)\text{CH}_3]^+$ . A is slightly more stable; B is the minimum nearest to the insertion transition state.

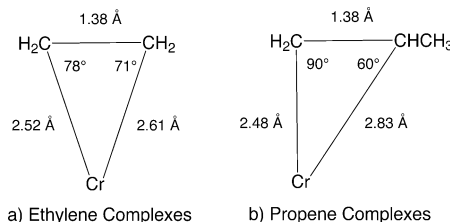


**Figure 3.** Average bond lengths and angles of four conformers of  $[\text{CpCr}(\text{THF})(\text{C}_2\text{H}_4)\text{Pr}]^+$  and six conformers of  $[\text{CpCr}(\text{THF})(\text{C}_3\text{H}_6)\text{Pr}]^+$ .



**Table 2.** Selected Internuclear Distances (Å) at the Insertion Transition States<sup>a</sup>

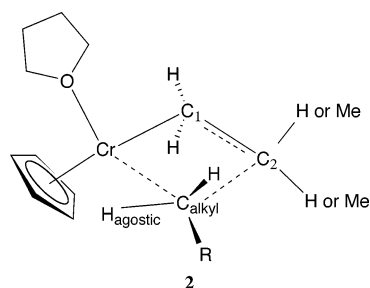
	[CrMe] <sup>+</sup>		[CrPr] <sup>+</sup>	
	+ethylene	+propene	+ethylene	+propene
Cr–C(alkyl)	2.205	2.206	2.226	2.224
C(alkyl)–C2	2.163	2.154	2.215	2.220
C2–C1	1.442	1.457	1.439	1.451
Cr–C1	2.125	2.094	2.132	2.104
Cr–C2	2.410	2.467	2.380	2.452
Cr–H <sub>agostic</sub>	2.295	2.273	2.192	2.158
H <sub>agostic</sub> –C(alkyl)	1.113	1.114	1.118	1.119

<sup>a</sup> C2 is the methyl-substituted carbon in the propene reactions.

propene coordination shows a distinct asymmetry in the binding of the two olefinic carbons, with the substituted carbon, C2, being about 0.35 Å farther from the chromium than C1 (Figure 3). The Cr–C1–C2 angle is typically about 90° in these complexes.

Although it is not a relevant intermediate in polymerization, a calculation of [CpCr(THF)(C<sub>2</sub>H<sub>4</sub>)]<sup>+</sup>, formed from the  $\pi$ -complex by loss of the alkyl group, lets us estimate the strength of the Cr–C bond to the alkyl ligand in the parent  $\pi$ -complex. Homolytic cleavage of the chromium-alkyl bond leaves the metal as high-spin Cr(II). We estimate the bond dissociation enthalpies to be about 29 kcal/mol for [Cr(C<sub>2</sub>H<sub>4</sub>)Me]<sup>+</sup> and about 22 kcal/mol for [Cr(C<sub>2</sub>H<sub>4</sub>)Pr]<sup>+</sup>. This difference in Cr–C bond strengths serves as a warning against using a methyl group as a model for a polymer chain and as a justification for taking at least the step to a propyl group.

**Transition States.** During the ethylene insertion reactions, the  $\alpha$ -carbon of the migrating alkyl group in the reactant becomes the  $\gamma$ -carbon of a lengthened product alkyl group (2). In the transition state for these



reactions, the C=C bond lengthens as the olefin moves toward the chromium-alkyl bond (Table 2). The  $\alpha$ -carbon of the alkyl ligand pivots to meet the olefin, causing one of the alkyl  $\alpha$ -hydrogen atoms to move closer to chromium. A weak agostic interaction is present in the transition state, judging by the fact that the Cr–H distances ( $\sim 2.2$  Å) are similar to that in the  $\gamma$ -agostic form of [CrPr]<sup>+</sup>.

In the optimized transition state structures (Figure 4), the three principal carbon atoms, the chromium and the newly agostic  $\alpha$ -hydrogen are nearly coplanar. Strict coplanarity would require the  $\beta$ - and  $\gamma$ -carbons to approach each other with their pendant atoms eclipsed. Instead, both the olefin and the migrating carbon rotate slightly. Rotation of the olefin breaks the coplanarity of the four heavy atoms. More notable is the rotation of the migrating carbon about the Cr–C <sub>$\alpha$</sub>  bond, which moves the agostic hydrogen atom out of the common plane, and renders its other two substituents sterically inequivalent. One substituent leads the migrating carbon as it advances toward the olefin, and the other

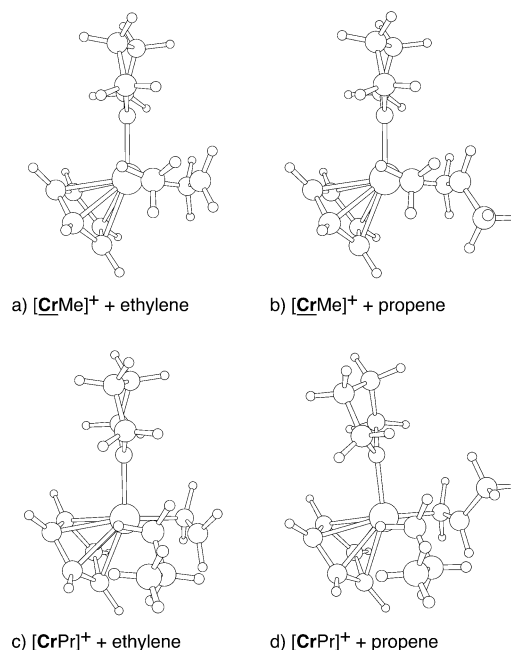


**Figure 4.** Optimized structures of insertion transition states: top row, methyl complexes; bottom row, propyl complexes; left, ethylene; right, propene. In each case, the migrating alkyl group is to the left of the figure, with the agostic hydrogen in front of the chromium and the olefin to the right. Only the lowest energy transition structure for each reaction is shown.

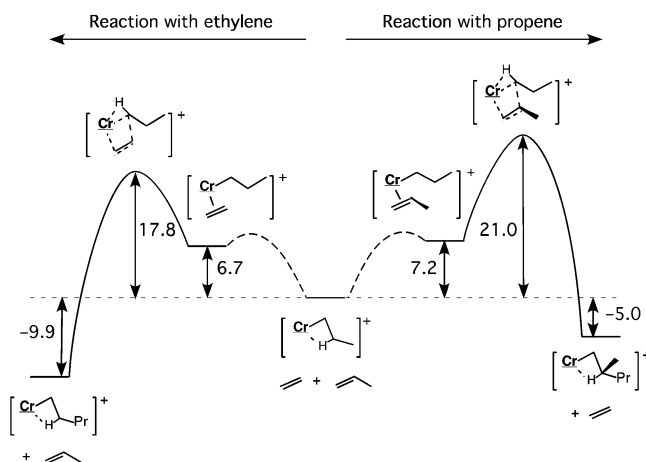


**Figure 5.** Gas-phase free energy changes for reactions of [CrPr]<sup>+</sup> with either ethane or propene, and the other alkene as spectator. The curves along the reaction path to formation of the  $\pi$ -complexes are dashed to indicate that the activation barriers for this step have not been calculated.

flanks it. A growing polymer chain (here approximated by an ethyl group) always occupies the flanking position (2).

The propene insertion transition states are similar to those for ethylene (Table 2 and Figure 5), and the tendency toward coplanarity of the chromium and three carbon atoms is stronger. For the transition states corresponding to normal 1,2-insertions examined in this study, the alkyl group migrates to the 2-carbon of propene. Propene can bind to the chromium atom via either of its two faces, leading to two diastereomeric transition states, and, in general, to two stereochemically different products. In the case of its reaction with [CrMe]<sup>+</sup>, two transition states were located with energies that differ by only 1 kcal/mol. In the lower energy structure, the methyl group of propene avoids the

**Table 3. Calculated Energies and Free Energies (kcal/mol, Relative to Separated Reactants) of Intermediates and Products<sup>a</sup>**

		$\pi$ -complex	insertion TS	product	
				$\gamma$ -agostic	$\beta$ -agostic
[CrMe] <sup>+</sup> + C <sub>2</sub> H <sub>4</sub>	$\Delta E_{298}(\text{gas})$	-8.6	+2.4 (11.0)	-17.0	-22.2
	$\Delta G_{298}(\text{gas})$	+3.2	+15.7	-4.3	-9.8
	$\Delta G_{298}(\text{CH}_2\text{Cl}_2)$	+5.6	+18.1	-0.9	-6.5
[CrMe] <sup>+</sup> + C <sub>3</sub> H <sub>6</sub>	$\Delta E_{298}(\text{gas})$	-9.9	+3.1 (13.0)	-16.6	-20.7
	$\Delta G_{298}(\text{gas})$	+2.8	+18.1	-1.6	-5.9
	$\Delta G_{298}(\text{CH}_2\text{Cl}_2)$	+8.0	+22.4	+3.3	-1.0
[CrPr] <sup>+</sup> + C <sub>2</sub> H <sub>4</sub>	$\Delta E_{298}(\text{gas})$	-3.7	+5.8 (9.4)	-16.1	-20.9
	$\Delta G_{298}(\text{gas})$	+6.7	+17.8	-5.1	-9.9
	$\Delta G_{298}(\text{CH}_2\text{Cl}_2)$	+7.9	+18.6	-4.4	-9.1
[CrPr] <sup>+</sup> + C <sub>3</sub> H <sub>6</sub>	$\Delta E_{298}(\text{gas})$	-4.1	+7.7 (11.8)	-12.9	-17.1
	$\Delta G_{298}(\text{gas})$	+7.2	+21.0	-1.2	-5.0
	$\Delta G_{298}(\text{CH}_2\text{Cl}_2)$	+10.3	+23.9	+1.8	-2.1

<sup>a</sup> Barrier heights in parentheses are relative to the  $\pi$  complex.

advancing hydrogen (Figure 4), while in the second structure (not shown, but see structure **2**), these groups approach each other. For propene insertion in [Cr(C<sub>3</sub>H<sub>6</sub>)-Pr]<sup>+</sup>, three different transition structures were located. The two most favored of these, differ from each other by less than 1 kcal/mol. In both of them, the methyl group of propene approaches the advancing hydrogen (Figure 4), thereby avoiding contact with the bulkier ethyl group (which models the growing polymer chain). A third transition structure in which the methyl and ethyl groups are syn to each other was also located; this is about 2.5 kcal/mol higher in energy than the lowest energy transition state.

**Reaction Energetics.** The energies of the key intermediates and products for the four reactions discussed above are shown in Table 3. Incorporation of either ethylene or propene into a polymer chain is exothermic by around 20 kcal/mol, though propene incorporation is consistently less favorable than ethylene incorporation. In the case of ethylene, the two steps of building the "polymer" chain, starting from a methyl complex to give sequentially  $\beta$ -agostic propyl and then pentyl species, are quite similar in energy. This is unexpected since the first ethylene monomer adds to a coordinatively unsaturated complex and produces a new agostic bond in the product, while the second monomer adds to a complex that is already coordinatively saturated (by virtue of the agostic bond) and produces no new agostic bonds. The resolution of this puzzle is the finding, noted above, that the Cr-C<sub>Me</sub> bond is stronger than the Cr-C<sub>Pr</sub> bond. By coincidence, the difference in these bond strengths is nearly equal to the strength of the  $\beta$ -agostic Cr-H-C interaction, thus canceling each other. For propene, the cancelation is not as precise and there is thus a larger difference in energy for the two steps.

In contrast to the overall energetics, the binding energies for olefin to the methyl- and propylchromium complexes, [CrMe]<sup>+</sup> and [CrPr]<sup>+</sup>, are significantly different. This difference is due to the necessity, in the propyl complex, of disrupting the agostic bond. The gas phase binding energy to either complex of both ethylene and propene is slightly exoenergetic, and somewhat more so for propene. In contrast, the free energies of ethylene and propene binding are positive, due to the loss of translational and rotational entropy. The ethylene binding energy obtained here for the methyl complex agrees with an earlier report.<sup>10</sup> Barriers to forming the  $\pi$ -complexes from the separated reactants may well exist, but we did not search for them. For the propyl

complex, we expect that this barrier will be approximately the energy required to break the agostic bond. It will therefore be independent of whether the incoming monomer is ethylene or propene and not rate limiting.

The energies of the insertion transition states significantly exceed the energies of the reactants and of the  $\pi$ -complexes in all cases. The olefin complexes of [CrMe]<sup>+</sup> have somewhat higher insertion barriers (relative to the  $\pi$ -complexes) than do the corresponding complexes with [CrPr]<sup>+</sup>, consistent with a stronger Cr-alkyl bond in the methyl complexes. The calculated free energy barrier for the insertion of ethylene on both complexes is low enough for rapid reaction at room temperature, consistent with the high activity for ethylene polymerization catalyzed by the related Cp\* complex. The free energy barriers for the insertion reactions of propene are higher than for ethylene by about 3 kcal/mol in the gas phase and 5 kcal/mol in CH<sub>2</sub>Cl<sub>2</sub> solution.

Solvent and counterions can have large effects on the energetics of the polymerization reactions in some cases.<sup>6</sup> We find that solvation of the reactants in dichloromethane does affect the energetic profile of the reactions as noted in Table 3. Propene is more strongly solvated than ethylene by 1 kcal/mol, probably because propene has a dipole moment while ethylene has none. The transition state for propene insertion is more weakly solvated than the transition state for ethylene insertion, by 1 kcal/mol. This may be a result of the different sizes of the complexes, since the larger complex is expected to be less strongly solvated. Thus, compared with the gas-phase results, solvation in dichloromethane increases the free energy barrier for propene insertion by 2 kcal/mol more than for ethylene insertion. We have not attempted to include the tetraphenylborate counterion in our calculations, but we note that it possesses no halides, oxygens or alkyl groups that would form strong dative bonds to the chromium. In any case, our primary motivation is to understand the differences in insertion rates of the two monomers, and this will not be affected by competitive interaction with the counterion.

Our calculations of the model complexes in solution are in good agreement with experimental observations of the reactivity of **1**. The predicted values of the energy barrier (relative to the  $\pi$ -complex; see Table 3) for ethylene polymerization by [CrMe]<sup>+</sup> (11.0 kcal/mol) and [CrPr]<sup>+</sup> (9.4 kcal/mol) are in good agreement with the estimated experimental activation energy of  $8 \pm 1$  kcal/mol.<sup>14</sup> The calculated differences in free energy of the insertion transition states for the two olefins in the gas

phase (2.4–3.2 kcal/mol) are very close to the difference in free energy barriers of 3.1 kcal/mol calculated from the experimental reactivity ratio for the Union Carbide catalyst in hexane at 100 °C.<sup>2</sup> The observed lack of copolymerization can thus be attributed to the significantly higher barrier for propene insertion relative to ethylene insertion.<sup>14</sup> The calculated barrier for propene insertion is sufficiently modest, that some reaction with propene might be expected. Indeed, **1** does react with propene, producing only C<sub>3</sub> and C<sub>4</sub> species.<sup>14</sup> This suggests that chain-termination reactions can compete with propene insertion. A closely related complex, [Cp\*Cr(OEt)<sub>2</sub>CH<sub>2</sub>SiMe<sub>3</sub>]<sup>+</sup>[B(C<sub>6</sub>H<sub>3</sub>(CF<sub>3</sub>)<sub>2</sub>)<sub>4</sub>]<sup>−</sup> does produce propene oligomers (at a much slower rate than it polymerizes ethylene).<sup>23</sup> These observations are consistent with our prediction of a moderately higher barrier for propene insertion and the interpretation that chain termination rates are comparable to propene insertion rates.

Our calculations and simple kinetic considerations suggest that reversible (weak) olefin binding, together with a significantly higher barrier for propene insertion, account for the inability of **1** and the Union Carbide catalyst to copolymerize ethylene and propene.<sup>14</sup> Indeed, the free energy surface shown in Figure 5 depicts a classic Curtin–Hammett situation, leading to polymerization of ethylene only. Copolymerization with weakly bound  $\pi$ -complexes would require that the insertion barriers for both monomers be nearly equal. Alternatively, copolymerization would be possible with different barriers as long as the barrier to dissociation of the  $\pi$ -complex were higher than both barriers to insertion. In this case, dissociation of a monomer from the  $\pi$ -complex would be slower than the competing insertion reaction, and monomer binding would be followed almost invariably by insertion. Assuming that the activation barrier for binding the two monomers are very similar, there would be no step that discriminates against propene relative to ethylene in such cases. This latter scenario appears to describe reactivity of d<sup>8</sup> Ni and Pd catalysts,<sup>6</sup> but not d<sup>3</sup> CpCr catalysts.

Others have drawn similar conclusions about the reactivity of Cr(III). Jensen et al.<sup>10</sup> used DFT calculations (BPW91) to study a series of Cp(donor)CrCH<sub>3</sub><sup>+</sup> complexes and estimated ethylene binding energies between 11 and 20 kcal/mol. Although the insertion barriers are low, the insertion transition states lie above the separated reactants in free energy in all cases, so reversible olefin binding is expected also for these Cr(III) catalysts and copolymerization is likely to be disfavored. Schmid and Ziegler predict stronger olefin binding to d<sup>2</sup> complexes than to d<sup>3</sup> complexes.<sup>24</sup> For two cationic propyl–Cr(IV) (high-spin, near-tetrahedral, d<sup>2</sup>) complexes containing bis-siloxy or bis-alkylamino ligands, they predict ethylene to bind with  $-\Delta E$  of 18 and 23 kcal/mol;<sup>11</sup> these numbers can be compared to 3.7 kcal/mol for [CrPr]<sup>+</sup>. Schmid and Ziegler find low barriers to insertion, which leads to the expectation that, for these Cr(IV) catalysts, olefin binding will be irreversible and insertion will usually follow. One might expect, therefore, that Cr(IV) catalysts may copolymerize ethylene and propene.<sup>25</sup> If so, they may make good functional models for the Phillips catalyst, which does copolymerize ethylene and propene, and whose chromium ligands probably include oxygen atoms derived from the silica surface. Furthermore, recent results from our laboratory suggest that cationic Cr(III) alkyls sup-

ported by  $\beta$ -diketiminato ligands (“nacnac”) are also capable of copolymerizing ethylene and  $\alpha$ -olefins.<sup>26</sup>

## Conclusion

Our results indicate that **1** (and, by analogy, the Union Carbide catalyst) does not copolymerize propene and ethylene because olefin binding is weak and reversible and because the barrier to propene insertion is higher than that for ethylene insertion. It is clear from this work that propene  $\pi$ -complexation is energetically accessible. However, this does not lead to propene polymerization because the activation barrier for insertion is too high, relative to the barriers for competing reactions (dissociation of the  $\pi$ -complex and, perhaps, chain termination). Thus, the higher insertion barrier for propene than for ethylene accounts for the failure of the catalyst to polymerize  $\alpha$ -olefins, either alone or with ethylene. Both steric repulsion and differential solvation effects contribute to the higher barrier for propene insertion.

Agostic interactions figure prominently in the reaction energetics of the methyl ([CrMe]<sup>+</sup>) and propyl ([CrPr]<sup>+</sup>) complexes. The propyl complex has agostic bonds between the metal and the propyl group and a weaker Cr–C(alkyl) bond. For this reason, accurate kinetic modeling of polymerization cannot employ a methyl group as a model for the growing chain. Strong  $\beta$ -agostic interactions have been predicted, and their stabilities suggest that  $\beta$ -hydride elimination may be an important side reaction competing with polymerization, especially of propene. This is consistent with experimental evidence for an increase in termination caused by the enchainment of  $\alpha$ -olefins. Apparently, a tertiary C–H group is more susceptible to  $\beta$ -hydrogen elimination than a secondary one.<sup>27</sup>

**Acknowledgment.** This work has been supported by grants from the NSF (D.J.D.: CHE-9971241, K.H.T.: CHE-9876426) and the Chevron Phillips Chemical Co. (K.H.T.).

**Supporting Information Available:** Selected bond lengths and angles of **1** ([Cp\*Cr(THF)<sub>2</sub>CH<sub>3</sub>]BPh<sub>4</sub>), [Cr(THF)Me]<sup>+</sup>, and [CrMe]<sup>+</sup> obtained by X-ray crystallography and calculated bond lengths (Å) and angles (deg) for [CpCr(THF)C<sub>3</sub>H<sub>7</sub>]<sup>+</sup>. This material is available free of charge via the Internet at <http://pubs.acs.org>.

## References and Notes

- (1) Hogan, J. P.; Banks, R. L. U.S. Patent 2,825,721, 1958. McDaniel, M. P. *Adv. Catal.* **1985**, *33*, 47.
- (2) Karapinka, B. L. U.S. Patent 3,709,853, 1973. Karol, F. J.; Karapinka, G. L.; Wu, C.; Dow, A. W.; Johnson, R. N.; Carrick, W. L. *J. Polym. Sci., Part A-1* **1972**, *10*, 2621.
- (3) Theopold, K. H. *CHEMTECH* **1997**, *27*, 26.
- (4) Theopold, K. H. *Eur. J. Chem.* **1998**, *15*.
- (5) Niu S.; Hall, M. B. *Chem. Rev.* **2000**, *100*, 353.
- (6) Rappé, A. K.; Skiff, W. M.; Casewit, C. J. *Chem. Rev.* **2000**, *100*, 1435.
- (7) Cossee, P. *J. Catal.* **1964**, *3*, 80. Arlman, E. J.; Cossee, P. *J. Catal.* **1964**, *3*, 99.
- (8) Grubbs, R. H.; Coates, G. W. *Acc. Chem. Res.* **1996**, *29*, 85.
- (9) Jensen, V. R.; Børve, K. J. *Organometallics* **1997**, *16*, 2514.
- (10) Jensen, V. R.; Angermund, K.; Jolly, P. W.; Børve, K. J. *Organometallics* **2000**, *19*, 403.
- (11) Schmid, R.; Ziegler, T. *Can. J. Chem.* **2000**, *78*, 265.
- (12) Froese, R. D. J.; Musaev, D. G.; Morokuma, K. *THEOCHEM—J. Mol. Struct.* **1999**, *462*, 121.
- (13) Resconi, L.; Cavallo, L.; Fait, A.; Piemontesi, F. *Chem. Rev.* **2000**, *100*, 1253.

- (14) Thomas, B. J.; Noh, S. K.; Schulte, B. K.; Sendlinger, S. C.; Theopold, K. H. *J. Am. Chem. Soc.* **1991**, *113*, 893.
- (15) Frisch, M. J.; Trucks, G. W.; Schlegel, H. B.; Scuseria, G. E.; Robb, M. A.; Cheeseman, J. R.; Zakrzewski, V. G.; Montgomery, Jr., J. A.; Stratmann, R. E.; Burant, J. C.; Dapprich, S.; Millam, J. M.; Daniels, A. D.; Kudin, K. N.; Strain, M. C.; Farkas, O.; Tomasi, J.; Barone, V.; Cossi, M.; Cammi, R.; Mennucci, B.; Pomelli, C.; Adamo, C.; Clifford, S.; Ochterski, J.; Petersson, G. A.; Ayala, P. Y.; Cui, Q.; Morokuma, K.; Malick, D. K.; Rabuck, A. D.; Raghavachari, K.; Foresman, J. B.; Cioslowski, J.; Ortiz, J. V.; Baboul, A. G.; Stefanov, B. B.; Liu, G.; Liashenko, A.; Piskorz, P.; Komaromi, I.; Gomperts, R.; Martin, R. L.; Fox, D. J.; Keith, T.; Al-Laham, M. A.; Peng, C. Y.; Nanayakkara, A.; Gonzalez, C.; Challacombe, M.; Gill, P. M. W.; Johnson, B.; Chen, W.; Wong, M. W.; Andres, J. L.; Gonzalez, C.; Head-Gordon, M.; Replogle, E. S.; Pople, J. A. *Gaussian 98, Revision A.7*; Gaussian, Inc.: Pittsburgh, PA, 1998.
- (16) Becke, A. D. *J. Chem. Phys.* **1993**, *98*, 5648.
- (17) Lee, C.; Yang, W.; Parr, R. G. *Phys. Rev. B* **1988**, *37*, 785.
- (18) Stevens, W. J.; Basch, H.; Krauss, M. *J. Chem. Phys.* **1984**, *81*, 6026.
- (19) Stevens, W. J.; Krauss, M.; Basch, H.; Jasien, P. G. *Can. J. Chem.* **1992**, *70*, 612.
- (20) Barone, V.; Cossi, M. *J. Phys. Chem. A* **1998**, *102*, 1995.
- (21) Poli, R. *Chem. Rev.* **1996**, *96*, 2135.
- (22) Cacelli, I.; Keogh, D. W.; Poli, R.; Rizzo, A. *J. Phys. Chem. A* **1997**, *101*, 9801.
- (23) White, P. A.; Calabrese, J.; Theopold, K. H. *Organometallics* **1996**, *15*, 5473.
- (24) Schmid, R.; Ziegler, T. *Organometallics* **2000**, *19*, 2756.
- (25) Amor Nait Ajjou, J.; Scott, S. L.; Paquet, V. *J. Am. Chem. Soc.* **1998**, *120*, 415.
- (26) Theopold, K. H.; MacAdams, L. A.; Puttnual, C.; Buffone, G. P.; Rheingold, A. L. *Polym. Mater. Sci. Eng.* **2002**, *86*, 310.
- (27) (a) Hogan, J. P. *J. Polym. Sci. A1* **2000**, *8*, 2673. (b) White, P. A.; Calabrese, J.; Theopold, K. T. *Organometallics* **1996**, *15*, 5473.

MA035080G